Fragment Anisotropies in Neutron-, Deuteron-, and Alpha-Particle-Induced Fission*

R. B. LEACHMAN AND L. BLUMBERG†
Los Alamos Scientific Laboratory, Los Alamos, New Mexico
(Received 6 July 1964; revised manuscript received 12 October 1964)

Fragment anisotropies have been measured from fission of several compound nuclei each formed by two different projectile-target combinations: U^{234} by $n+U^{233}$ and $\alpha+Th^{230}$, U^{236} by $n+U^{235}$ and $\alpha+Th^{232}$, Np^{238} by $n+Np^{237}$ and $d+U^{236}$, Pu^{239} by $d+Np^{237}$ and $\alpha+U^{235}$, and Pu^{240} by $n+Pu^{239}$ and $\alpha+U^{236}$. These measurements extended over an energy range of approximately 12- to 25-MeV excitation energy of the compound nucleus. Transmission coefficients were calculated to estimate the mean-square orbital angular momentum $\langle l^2\rangle_{av}$ of the fissioning nuclei required for the theory of fragment angular distributions. At the higher energies attained in the present experiment, uncertainties in $\langle l^2\rangle_{av}$ introduced by Coulomb-barrier penetration effects were small, and it was therefore possible to make comparisons between measurements and theory which indicate that the distortion of the compound nucleus at the saddle-point configuration before fission is independent of the total angular momentum and the identity of the bombarding particle. At the lower energies, where the Coulomb parameter $\eta=Z_1Z_2e^2/\hbar v$ is roughly 15, this comparison has shown that calculations of transmission coefficients for alpha particles give values of $\langle l^2\rangle_{av}$ in agreement with the data only if careful attention is given to the effects of barrier penetration. At the lowest energies, comparisons of data from U^{236} and Pu^{240} indicate that the effect of target spin on fission anisotropy is small. Additional angular distributions from neutron-induced fission of Th^{232}, $U^{233,234,235,236,238}$, Np^{237}, and Pu^{239} and anisotropies of alpha-particle-induced fission of $U^{233,235,238}$ are also reported.

I. INTRODUCTION

STUDIES[1–7] of fragment anisotropy fom fission induced by particles of up to about 40 MeV have been rewarding in providing information about nuclei at the saddle-point deformation. A notable recent success has been the determination[8] of the unusually large pairing energy for the highly deformed nucleus before fission.

In the present study, we have measured fission anisotropies over a broad range of excitation energy for compound nuclei produced by two different target-projectile pairs: for example, the compound nucleus U^{236} produced by neutron irradiation of U^{235} and alpha-particle irradiation of Th^{232}. For each compound nucleus, the two principal factors affecting fission anisotropy are K_0^2 and the mean-square orbital angular momentum $\langle l^2\rangle_{av}=\sum(2l+1)l^2T_l/\sum(2l+1)T_l$; thus, anisotropy data from a compound nucleus formed by different target-projectile pairs allow comparison between the relative values of one of these factors if the relative values of the other factor can be established. The quantity K_0 is the standard deviation in the Gaussian distribution that is assumed for K, where K is the projection of the total angular momentum I on the nuclear symmetry axis. The projection K has significance in being the resultant of the orbital angular momentum and spins of the unpaired nucleons in the saddle-point nucleus. The quantity K_0 is related[9] to the deformation of the saddle-point nucleus through the effective moment of inertia $\mathcal{I}_{eff}=\hbar^2K_0^2/T$, where $\mathcal{I}_{eff}^{-1}=\mathcal{I}_{II}^{-1}-\mathcal{I}_{\perp}^{-1}$, $\mathcal{I}_{\perp}$, and $\mathcal{I}_{II}$ are components of the moment of inertia about axes perpendicular to and along the nuclear symmetry axis, respectively, and T is the nuclear temperature.

The leading terms of the classically derived expression for fission anisotropy[10] [defined as $W(0)/W(90)$, the ratio of 0° and 90° differential fragment cross sections] given by Leachman and Sanmann[11] are

$$\frac{W(0)}{W(90)}=1+\frac{\langle l^2\rangle_{av}}{4K_0^2}-\frac{\langle l^2\rangle_{av}I_0^2}{36K_0^4}+\frac{\langle l^2\rangle_{av}I_0^2}{3(1+p)\alpha^2K_0^2}. \quad (1)$$

Here, I_0 is the spin of the target nucleus. The relative probability Γ_f/Γ_n for fission compared to neutron de-

* Work performed under the auspices of the U. S. Atomic Energy Commission.
† Now at Oak Ridge National Laboratory, Oak Ridge, Tennessee.

[1] L. Blumberg and R. B. Leachman, Phys. Rev. **116**, 102 (1959).
[2] J. E. Simmons and R. L. Henkel, Phys. Rev. **120**, 198 (1960).
[3] J. E. Brolley, Jr., and W. C. Dickinson, Phys. Rev. **94**, 640 (1954); A. A. Varfolomeev, A. S. Romantseva, and V. M. Kutukova, Doklady Akad. Nauk SSSR **105**, 693 (1955) [English transl.: Atomic Energy Research Establishment Library Translation No. 707 (July 1956)]; R. L. Henkel and J. E. Brolley, Jr., Phys. Rev. **103**, 1292 (1956); A. N. Protopopov and V. P. Eismont, Zh. Eksperim. i Teor. Phys. **34**, 250 (1958) [English transl.: Soviet Phys.—JETP **34**, 173 (1958)]; A. Katase, Mem. Fac. Eng., Kyushu Univ. **21**, 81 (1961); and V. G. Nesterov, G. N. Smirenkin, and I. I. Bondarenko, At. Energ. (USSR) **10**, 620 (1961) [English transl.: Soviet J. At. Energy **10**, 613 (1961)].
[4] R. Vandenbosch, H. Warhanek, and J. R. Huizenga, Phys. Rev. **124**, 846 (1961).
[5] C. T. Coffin and I. Halpern, Phys. Rev. **112**, 536 (1958).
[6] G. L. Bate, R. Chaudhry, and J. R. Huizenga, Phys. Rev. **131**, 722 (1963).
[7] J. E. Simmons, R. B. Perkins, and R. L. Henkel, preceding paper, Phys. Rev. **137**, B809 (1965).
[8] J. J. Griffin, Phys. Rev. **132**, 2204 (1963).
[9] I. Halpern and V. M. Strutinski, in *Proceedings of the Second International Conference on the Peaceful Uses of Atomic Energy, Geneva, 1958* (United Nations, Geneva, 1959), Vol. 15, p. 408.
[10] The exact expression has been derived by J. J. Griffin, Phys. Rev. **127**, 1248 (1962). Equation (1) is based on a probability distribution in l increasing linearly with l to the maximum l, which is the classical case for neutrons. In Ref. 4 this has been shown to be adequate for the case of alpha particles.
[11] R. B. Leachman and E. E. Sanmann, Ann. Phys. (N. Y.) **18**, 274 (1962).

excitation[12] defines p and $\mathcal{C}^2$ by

$$\frac{\Gamma_f}{\Gamma_n}=p\exp\left[\frac{\hbar^2I^2}{2T}\left(\frac{1}{\mathcal{I}_n}-\frac{1}{\mathcal{I}_\perp}\right)\right]=p\exp\frac{I^2}{\mathcal{C}^2}, \qquad (2)$$

where $\mathcal{I}_n$ is the moment of inertia of the nucleus formed by neutron emission. Gilmore *et al.*[13] have obtained recent evidence in favor of this I-dependent fission probability from comparisons of fission cross sections with calculated $\langle l_2\rangle_{\rm av}$ values for cases where the same compound nuclei were formed by two different projectile-target combinations in heavy-ion-induced fission.

Fission anisotropy from the same compound nucleus produced by two different reactions allows three new studies based on Eq. (1):

(1) At higher energies where calculations of $\langle l^2\rangle_{\rm av}$ are reliable, the data allow a test of the usual assumption that K_0 (and thus the saddle-point deformation) is dependent only upon the excitation energy of the compound nucleus and is specifically independent of the total angular momentum I. For this test, terms involving I_0 in Eq. (1) are neglected. Use of reasonable values for moments of inertia have shown[10,11] these terms to be very small compared to the second term on the right in Eq. (1); these terms are certainly negligible for the low-spin case of $n+\mathrm{Pu}^{239}$ ($I_0=\frac{1}{2}$) and $\alpha+\mathrm{U}^{236}$. The quantity $\langle l^2\rangle_{\rm av}$ is rather well established for neutron bombardments because transmission coefficients T_l from classical,[14] square-well,[15] and optical-model[16] calculations are in excellent agreement with data. For alpha-particle bombardments, calculated T_l values result in reaction cross sections $\sigma_r=\pi\lambda^2\sum(2l+1)T_l$, where λ is the wavelength, in agreement with data[6,17,18] that are available for all but the lowest of the present energies.

(2) At lower energies, the relative $\langle l^2\rangle_{\rm av}$ values for the different projectiles are readily obtained from anisotropy data if K_0^2 has been established to be I independent. Fission thus allows determination of the angular momentum dependence of Coulomb barrier penetration at energies much lower than have been attained using other reactions. This is possible because rare fission events in the presence of large backgrounds from other reactions or from scattering can experimentally be distinguished by the distinctively large energy released in fission and large mass of the fragments. In the present measurements, charged particles with energies from about one-half to the full Coulomb barrier height were used, that is, 8.5–14.5-MeV deuterons and 16–29-MeV alpha particles. Jauho[19] has noted that these lowest alpha-particle energies are nearer the energies of spontaneously emitted alpha particles in radioactive decay than the energies of most reaction studies, and thus the present study of $\langle l^2\rangle_{\rm av}$ provides an interesting bridge between the energies for which WKB calculations are employed at low energies for alpha decay and the optical-model[20] and square-well calculations[15] used at high energies in nuclear-reaction analyses.

(3) For cases where the target nuclei have different spins I_0, the effect of target spin on anisotropy can be tested without the ambiguity inherent in previous tests of this effect,[1,2] where anisotropies from different compound nuclei were compared ($n+\mathrm{U}^{233}$, $n+\mathrm{U}^{235}$, and $n+\mathrm{Pu}^{239}$). This target-spin effect arises from several possible causes. Bohr[21] has noted that increasing target spin I_0 should reduce the anisotropy, as is seen by the negative sign of the third term on the right in Eq. (1). However, the data[1,2] indicate that causes with opposite sign are dominant. Mottelson[22] suggested that increasing target spin would increase the probability for fission, as seen by Eq. (2), and thus increase the anisotropy. However, this effect requires an anomalously small moment of inertia $\mathcal{I}_n$ [small $\mathcal{C}^2$ in Eq. (2) and in the positive, last term of Eq. (1)] to fit the data. Strutinski[23] has suggested a K distribution deviating from the Gaussian distribution assumed in the derivation of Eq. (1), but this has been shown[11] to be inadequate to explain the observed effect. Finally, Huizenga[24] noted that a decrease of K_0 (a decrease in $\mathcal{I}_{\rm eff}$ resulting from a larger saddle-point deformation) for U^{235} relative to Pu^{239} tends to explain the observed anisotropy differences simply by the second term in Eq. (1); the $\mathcal{I}_{\rm eff}$ values subsequently calculated from the liquid-drop model[25] indeed indicated that about one-half of the observed effect can be so explained. However, the liquid-drop model at present provides only a qualitative picture of the asymmetric fission of heavy nuclei, and thus an experimental

[12] G. A. Pik-Pichak, Zh. Eksperim. i Teor. Phys. **36**, 961 (1959) [English transl.: Soviet Phys.—JETP **9**, 679 (1959)].

[13] J. Gilmore, S. G. Thompson, and I. Perlman, Phys. Rev. **128**, 2276 (1962).

[14] J. M. Blatt and V. F. Weisskopf, *Theoretical Nuclear Physics* (John Wiley & Sons, Inc., New York, 1952), p. 319.

[15] Reference 14, p. 360.

[16] J. R. Beyster, R. G. Schrandt, M. Walt, and E. W. Salmi, Los Alamos Scientific Laboratory Report LA-2099, 1956 (unpublished).

[17] R. Vandenbosch, T. D. Thomas, S. E. Vandenbosch, R. A. Glass, and G. T. Seaborg, Phys. Rev. **111**, 1358 (1958); J. Wing, W. J. Ramler, A. L. Harkness, and J. R. Huizenga, *ibid.* **114**, 163 (1959); R. Gunnink and J. W. Cobble, *ibid.* **115**, 1247 (1959); B. M. Forman, Jr., W. M. Gibson, R. A. Glass, and G. T. Seaborg, *ibid.* **116**, 382 (1959); and L. J. Colby, Jr., M. L. Shoaf, and J. W. Cobble, *ibid.* **121**, 1415 (1961).

[18] G. P. Ford and R. B. Leachman, following paper, Phys. Rev. **137**, B826 (1965).

[19] P. Jauho (private communication). We are grateful to Professor Jauho for this interesting suggestion.

[20] J. R. Huizenga and G. Igo, Nucl. Phys. **29**, 462 (1962) and Argonne National Laboratory Report 6373, 1961 (unpublished).

[21] Aa. Bohr, in *Proceedings of the International Conference on the Peaceful Uses of Atomic Energy, Geneva, 1955* (United Nations, New York, 1956), Vol. 2, p. 151.

[22] B. R. Mottelson (private communication).

[23] V. M. Strutinski, Zh. Eksperim. i Teor. Phys. **39**, 781 (1960) [English transl.: Soviet Phys.—JETP **12**, 546 (1961)]; Nucl. Phys. **27**, 348 (1961); and Zh. Eksperim. i Teor. Phys. **40**, 933 (1961) [English transl.: Soviet Phys.—JETP **13**, 652 (1961)].

[24] J. R. Huizenga (private communication). Also see W. R. Gibbs and J. J. Griffin, Phys. Rev. **137**, B807 (1965) (this issue).

[25] S. Cohen and W. J. Swiatecki, Ann. Phys. (N. Y.) **22**, 406 (1963).

test of the change in anisotropy with target spin for the same compound nucleus (fixed K_0) is of interest.

II. EXPERIMENTAL

Data were obtained by two different methods during the course of the experimental program. A catcher foil technique was employed for angular-distribution measurements of neutron- and alpha-particle-induced fission. Semiconductor detectors were used for additional anisotropy measurements of alpha- and deuteron-induced fission.

A. Catcher Foil Measurements

The experiment for neutron irradiations was similar to that previously employed.[1] All targets were greater than 93% in isotopic abundance. For neutron-induced fission of Th^{232}, U^{233}, U^{235}, U^{238}, and Pu^{239}, thick targets were used; otherwise, target deposits from 160 $\mu g/cm^2$ to 2.3 mg/cm^2 on backings of 0.1–1.1-mg/cm^2 Ni or 1.4-mg/cm^2 Au were used.

A $D(d,n)He^3$ neutron source was utilized for neutrons in the energy range $9 \lesssim E_n \lesssim 12$ MeV. Deuterium gas cells of 2 or 3 cm length at pressures of 11 to 15 atm were used with external beams of typically 10μA from the cyclotron entering through double-foil[26] windows of 0.0003-in. and 0.001-in. molybdenum, between which a high velocity hydrogen coolant was provided. A $T(p,n)He^3$ neutron source of similar construction with 8 atm tritium pressure was used for 5-MeV neutrons. At energies below 5 MeV, a $T(p,n)He^3$ source with one uncooled 0.0003-in. molybdenum window and 4 atm of tritium was used with a beam from the Van de Graaff accelerator. Neutron energies in the range $13.4 \leqq E_n \leqq 15$ MeV were obtained with the $T(d,n)He^4$ reaction at the Cockcroft-Walton accelerator.

Irradiations were performed with the target gas removed to measure the number of fission events and the associated fragment angular distributions resulting from background neutrons from (d,n) and (d,np) reactions on the structural material of the neutron source. Corrections for this background were applied to all data obtained with the $D(d,n)$ source. Irradiations were also performed at each neutron energy with the fission source removed to measure neutron-induced beta activity in the catcher foils. Calibration irradiations for each thick fission source were performed using thermal neutrons, which produce fission isotropy. For the partially thick Np^{237} source, the data were normalized to those of Simmons and Henkel[2] at $E_n = 8$ MeV.

For alpha-particle-induced fission with the catcher foil method, the larger flux of alpha particles, compared to neutrons, permitted an improvement in the angular resolution for irradiations with alpha-particle energies $E_\alpha > 19$ MeV. Catcher "wheels" with 1-cm diam apertures were used with wheel diameters of 6 cm for neutron irradiations and 18 cm for alpha-particle irradiations. The average angles θ of the apertures used were 7.2°, 24°, 40.5°, 57°, and 90° and $\pi+\theta$. The data at $E_\alpha = 18.2$ MeV were obtained with a catcher wheel of 6 cm diam and with catcher apertures at $\theta = 21.3°$, 90°, and $\pi+\theta$. In both cases, the external alpha-particle beam of the cyclotron was collimated to 0.64 cm diam and irradiated the fission source through apertures in the catcher wheels at $\theta = 0°$ and 180°. Irradiations were of 1 to 14 h duration at beam currents of approximately 0.15 to 0.6 μA. The principal experimental difficulty encountered in these irradiations was the presence of an appreciable background beta activity on the catcher foils due to recoil activity from the source and structural materials, as well as activity induced in the catcher foils by the scattered beam. The background activities were clearly discernible from the time variation of the ratios of the beta activities from the catchers at different angles, and it was therefore necessary to wait for approximately 5 to 14 h after an irradiation for these ratios to become constant before recording data. The thick-source calibration factors for Th^{232} and U^{236} fission source foils for alpha-particle energies below 22 MeV were obtained by comparison to thin-source results at higher energies. These and other effects relevant to the experimental procedure and corrections applied to the data are discussed in more detail elsewhere.[27]

B. Semiconductor Detector Data

Many of the alpha-particle measurements and all of the deuteron-induced fission anisotropy data were obtained with two 300-Ω-cm gold-surface barrier detectors with 1.4-cm apertures positioned at laboratory angles $\theta = 90°$ and 174° relative to the beam direction. The electronics were similar to that employed by Vandenbosch *et al.*[4] The counters were 11.2 cm from the fission source foil, and the beam was collimated to 0.16 cm in the plane of the scattering and 0.4 cm high. The chamber was calibrated with a spontaneous Cf^{252} fission source to correct for slightly unequal solid angles subtended by the 90° and 174° counters. Data were corrected for backgrounds of less than 1 count/min from Cf^{252} contamination on the counters. Irradiations were performed for several orientations of the fission source to determine whether the effective center of the source coincided with the geometric center of the scattering chamber; anisotropy variations of about 2% noted in these tests are included in the quoted uncertainties.

Measurements at 16–17-MeV alpha-particle energy were of particular interest since the (α,f) reaction is the only fission process energetically possible at these energies. Therefore, special effort went into these irradiations. The low-fission cross sections, which are of the order of 1 μb, resulted in only about 1 observed fission/min. With conventional microsecond electronics, alpha-particle pileup caused a tail extending into the

[26] R. Nobles, Rev. Sci. Instr. 28, 962 (1957).

[27] L. Blumberg, thesis, Columbia University, 1962 (unpublished).

TABLE I. Relative angular distributions $W(\theta)/W(90)$ of fission-fragment activities for neutron irradiations. Measurements were by catcher foil techniques.

Neutron energy (MeV)	$W(0)/W(90)$	$W(22.5)/W(90)$	$W(45)/W(90)$	$W(67.5)/W(90)$
		U^{233}		
9.47±0.23	1.30±0.02	1.21±0.02	1.13±0.02	1.04±0.02
10.84±0.24	1.23±0.02	1.15±0.02	1.10±0.02	1.00±0.02
11.81±0.24	1.20±0.02	1.11±0.02	1.09±0.02	0.97±0.02
11.84±0.22	1.20±0.02	1.10±0.02	1.06±0.02	0.98±0.02
		U^{234}		
9.07±0.20	1.44±0.03	1.36±0.03	1.16±0.03	1.09±0.03
9.53±0.24	1.42±0.04	1.35±0.03	1.23±0.03	1.07±0.03
10.80±0.24	1.28±0.03	1.27±0.03	1.11±0.02	1.08±0.02
11.84±0.23	1.26±0.03	1.27±0.03	1.12±0.02	1.05±0.03
13.4 ±0.2	1.27±0.05		1.17±0.04	
14.1 ±0.1	1.22±0.03		1.06±0.02	
14.95±0.40	1.23±0.03		1.08±0.03	
		U^{235}		
0.7 ±0.1	1.16±0.02	1.10±0.02	1.11±0.02	1.06±0.02
1.5 ±0.1	1.13±0.02	1.07±0.02	1.08±0.02	1.04±0.02
2.6 ±0.1	1.17±0.02	1.11±0.02	1.08±0.01	1.01±0.01
3.97±0.05	1.18±0.02	1.13±0.02	1.10±0.02	1.04±0.02
4.68±0.10	1.23±0.03	1.18±0.03	1.16±0.03	1.04±0.03
9.04±0.20	1.35±0.02	1.25±0.02	1.16±0.02	1.13±0.02
9.53±0.24	1.35±0.02	1.25±0.02	1.18±0.02	1.13±0.02
10.71±0.26	1.29±0.02	1.19±0.02	1.15±0.02	1.11±0.02
11.88±0.23	1.28±0.02	1.19±0.02	1.19±0.02	1.12±0.02
11.97±0.19	1.28±0.02	1.22±0.02	1.18±0.02	1.12±0.02
13.4 ±0.2	1.26±0.02	1.22±0.02	1.14±0.02	1.05±0.02
14.1 ±0.1	1.29±0.01	1.22±0.01	1.14±0.01	1.05±0.01
14.95±0.40	1.29±0.02	1.26±0.02	1.14±0.02	1.06±0.01
		U^{236}		
9.04±0.20	1.48±0.04	1.35±0.03	1.17±0.03	1.04±0.03
9.67±0.22	1.41±0.04	1.33±0.04	1.18±0.05	1.06±0.04
10.79±0.24	1.35±0.03	1.30±0.03	1.15±0.03	1.05±0.03
11.88±0.23	1.31±0.04	1.27±0.03	1.16±0.03	1.03±0.03
13.4 ±0.2	1.36±0.07		1.05±0.06	
14.1 ±0.1	1.25±0.03		1.07±0.03	
14.95±0.40	1.38±0.06	1.29±0.07	1.10±0.05	1.08±0.05
		U^{238}		
5.04±0.10	1.20±0.02	1.17±0.02	1.09±0.02	0.98±0.02
7.91±0.25	1.54±0.03	1.39±0.03	1.19±0.03	1.06±0.04
9.09±0.20	1.39±0.02	1.31±0.02	1.16±0.03	1.06±0.04
9.61±0.23	1.38±0.02	1.26±0.02	1.15±0.03	1.08±0.04
10.84±0.24	1.29±0.02	1.24±0.02	1.12±0.02	1.08±0.04
11.91±0.21	1.26±0.02	1.23±0.02	1.13±0.03	1.10±0.05
13.4 ±0.2	1.27±0.02		1.10±0.03	
14.1 ±0.1	1.31±0.02		1.14±0.02	
14.95±0.40	1.33±0.02	1.22±0.02	1.15±0.02	1.02±0.02
		Pu^{239}		
9.53±0.24	1.24±0.02	1.19±0.02	1.13±0.02	1.04±0.02
10.79±0.24	1.19±0.02	1.16±0.02	1.11±0.02	1.06±0.01
11.83±0.22	1.17±0.02	1.13±0.02	1.11±0.02	1.04±0.02
11.83±0.22	1.20±0.02	1.16±0.02	1.10±0.02	1.05±0.02
		Th^{232}		
5.09±0.11	1.21±0.04	1.26±0.04	1.08±0.03	1.00±0.03
8.96±0.20	1.69±0.05	1.52±0.04	1.24±0.03	1.07±0.03
9.61±0.23	1.54±0.05	1.43±0.04	1.22±0.04	1.06±0.03
10.74±0.24	1.41±0.04	1.36±0.03	1.16±0.03	1.02±0.03
11.82±0.22	1.41±0.04	1.33±0.03	1.14±0.03	1.07±0.03
13.4 ±0.2	1.38±0.06		1.09±0.04	
14.1 ±0.1	1.40±0.04		1.12±0.03	
14.95±0.40	1.50±0.04	1.45±0.03	1.21±0.03	1.02±0.03
		Np^{237}		
8.98±0.20	1.18±0.05	1.18±0.05	1.09±0.04	1.05±0.04
9.62±0.23	1.21±0.05	1.18±0.04	1.11±0.04	1.05±0.04
10.79±0.24	1.21±0.05	1.22±0.04	1.14±0.04	1.10±0.04
11.80±0.22	1.23±0.05	1.17±0.05	1.14±0.04	1.09±0.04
13.4 ±0.2	1.17±0.07		1.03±0.06	
14.1 ±0.1	1.12±0.05		1.04±0.04	
14.95±0.40	1.16±0.05		1.08±0.04	

energy spectrum of fragments at these lowest energies, even though a minimum depletion depth in the counters was used. To reduce these difficulties, additional runs were made with larger solid angles and with faster electronics. The distance from fission source to detectors was 12.2 cm, the 174° detectors were an array of four 1-cm×1-cm detectors, and the 90° detectors were two circular 4.5-cm² detectors. To reduce pileup, use was made of amplifiers[28] which passed in 30-nsec resolving time only those pulses exceeding the energies of scattered alpha particles. Still some low-energy tail in the energy spectrum remained, and this was attributed to heavy ions from reactions on light elements in the target.[29] Corrections for these tails extending into the fragment spectrum are discussed later.

III. RESULTS

The data consist of ratios of fragment beta activity for the catcher foil measurements and of ratios of fragment counts for the semiconductor detector results. After background and calibration corrections and transformation to the center-of-mass (c.m.) system, the resulting ratios are identical to the c.m. differential cross section ratios $W(\theta)/W(90)$ at c.m. angle θ. Symmetry about $\theta=90°$ is assumed in the data analysis, consistent with measurements of Leachman and Ford[30] for 14-MeV neutron-induced fission.

A. Catcher Foil Data

Angular distribution results are summarized in Table I for neutron-induced fission and in Table II for alpha-particle-induced fission. Uncertainties in the data are standard deviations resulting from counting statistics and uncertainties introduced by the following corrections: (1) proportional-counter natural background of about 10 counts/min which were generally less than 5% of the total counts; (2) variations of $\lesssim 1\%$ in relative counter efficiency; (3) neutron-induced activity in the catchers resulting in corrections of $\lesssim 5\%$ to the activity ratios; (4) for effects introduced by use of

[28] The circuits were designed by R. D. Hiebert and J. S. Lunsford (1964) and were similar to the circuit described by A. Barna and J. H. Marshall, Rev. Sci. Instr. **35**, 881 (1964).

[29] C. Zafiratos, Phys. Rev. **136**, B1279 (1964).

[30] R. B. Leachman and G. P. Ford, Nucl. Phys. **19**, 366 (1960).

TABLE II. Relative angular distributions $W(\theta)/W(90)$ of fission-fragment activities for alpha-particle irradiations. Measurement was by catcher foil techniques.

Alpha-particle energy MeV)	$W(7.2)/W(90)$	$W(24)/W(90)$	$W(40.5)/W(90)$	$W(57)/W(90)$
		Th^{232}		
16.95±0.29		1.40±0.05[a]		
18.06±0.32		1.23±0.02[a]		
19.06±0.30	1.31±0.02	1.24±0.02	1.17±0.02	1.12±0.02
20.67±0.28	1.26±0.02	1.17±0.02	1.16±0.02	1.10±0.02
21.85±0.09	1.26±0.02	1.21±0.02	1.15±0.02	1.07±0.02
22.97±0.07	1.24±0.02	1.17±0.02	1.11±0.02	1.05±0.02
24.22±0.04	1.35±0.02	1.24±0.02	1.16±0.02	1.08±0.02
25.50±0.02	1.51±0.02	1.33±0.02	1.16±0.01	1.07±0.01
26.88±0.22	1.56±0.02	1.35±0.02	1.19±0.02	1.07±0.02
28.67±0.02	1.57±0.02	1.41±0.01	1.24±0.01	1.08±0.01
		U^{236}		
17.05±0.20		1.42±0.05[a]		
17.91±0.21		1.13±0.03[a]		
19.15±0.20	1.21±0.02	1.14±0.02	1.08±0.02	1.02±0.02
20.73±0.18	1.17±0.02	1.12±0.02	1.06±0.01	1.03±0.01
22.92±0.04	1.14±0.01	1.11±0.01	1.04±0.01	1.01±0.01
24.31±0.03	1.17±0.01	1.12±0.01	1.05±0.01	1.01±0.01
25.64±0.05	1.25±0.01	1.14±0.01	1.09±0.01	1.04±0.01
26.71±0.04	1.27±0.01	1.20±0.01	1.10±0.01	1.03±0.01
28.63±0.03	1.33±0.01	1.22±0.01	1.14±0.01	1.08±0.01

[a] $\theta=21.3°$ for indicated irradiations.

thick fission sources, calibration corrections of $\lesssim 9\%$ as inferred from thermal-neutron irradiations for the neutron data and from comparisons to thin target results for the alpha-particle data; (5) displacement of the effective source position from the center of the scattering chamber because of nonuniformity of source deposit and incident beam flux, which results in $\lesssim 0.4\%$ corrections to anisotropies; (6) breakup neutrons from $D(d,np)$ and from other materials in the target contribute 2.3 to 59% and 2.6 to 23.8%, respectively, of the total fissions observed from $9 \leqq E_n \leqq 12$, but the use of known $D(d,np)$ and $D(d,n)$ cross sections[31] result in calculated corrections of $\lesssim 4.5\%$ for the combined effects; and (7) fissionable impurities in the fission sources, for which anisotropy corrections of $\lesssim 0.7\%$ were required.

The kinematic transformation from laboratory to c.m. cross section was evaluated by assuming that the most probable mass division $M_H/M_L \approx 1.46$ and total kinetic energy release $E_T \approx 165$ MeV observed for thermal-neutron fission of U^{235} also pertain to our irradiations. The effective laboratory angles for fragment detection differed significantly from the mean geometric angles only for the $\theta=0°$ catcher foil in the neutron data, for which $\theta_{rms} \approx 6.8°$. An additional rms angular spread of about 5.6°, introduced by the angle distribution of neutrons impinging on the fission source, increased the effective laboratory angle to $\approx 8.8°$. The average c.m. angles were essentially equal to the effective laboratory angles for the experiments where data at θ and $\pi+\theta$ are combined, except that $\theta_{lab}=90°$ corresponds to $\theta_{c.m.}=91°$ for the neutron data with $E_n \gtrsim 9$ MeV and $\theta_{c.m.}=93°$ for the alpha-particle data.

Neutron energies in Table I are mean values weighted with respect to the calculated neutron energy distribution at the fission source. Energy spreads are rms deviations from the weighted mean. Since a gaseous source was used, the calculations of the spreads included effects of multiple scattering, energy loss, and energy straggling of the accelerator beam in the windows of the gas target, energy loss in the gas, and the differential cross sections for the neutron-producing reactions.[31] To evaluate the mean energy and energy spread, multiple integration was performed over the window area, gas volume, and fission source area by a

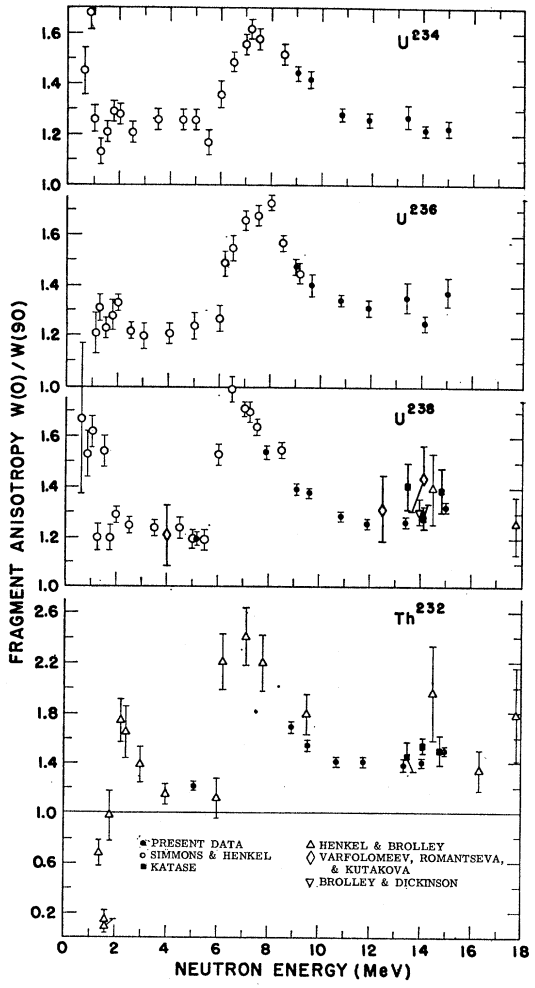

FIG. 1. Anisotropy of fragments from neutron-induced fission of even-even isotopes. Angles for the present data were actually 9° and 91°. See Refs. 2 and 3 for earlier data.

[31] L. Cranberg, A. Armstrong, and R. L. Henkel, Phys. Rev. 104, 1639 (1956); J. L. Fowler and J. E. Brolley, Jr., in *Fast Neutron Physics*, edited by J. B. Marion and J. L. Fowler (Interscience Publishers, Inc., New York, 1959); W. E. Wilson, D. B. Fossan, and R. L. Walter, Bull. Am. Phys. Soc. 5, 410 (1960), and private communication.

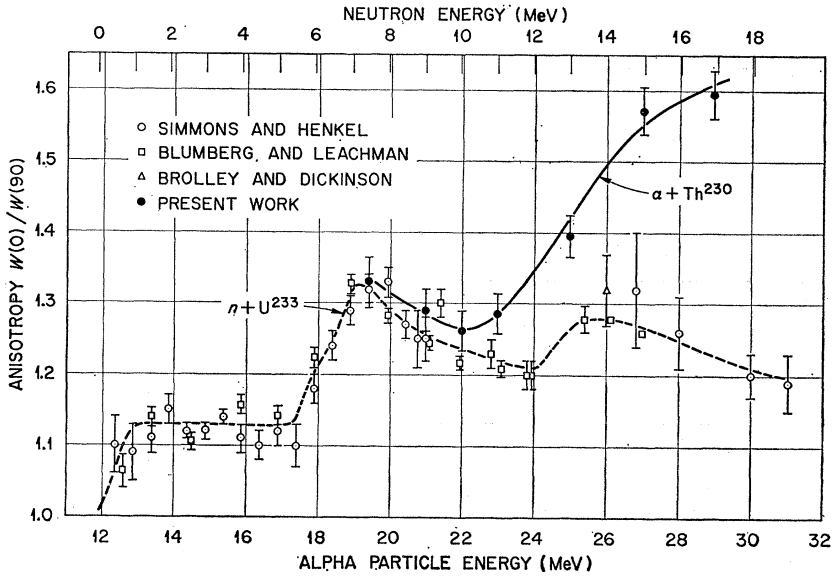

FIG. 2. Anisotropy data of fragments from the compound nucleus U^{234}. Curves are not fits to the data. The angles for the present data were actually 6° and 93° for alpha particles and 9° and 91° for neutrons. See Refs. 1–3 for earlier data.

Monte Carlo technique. For cyclotron irradiations, the beam energy was measured with an energy monitoring system previously reported.[32] Alpha-particle energies in Table II are average beam energies in the fission source. The spread in the energy of the cyclotron beam was about 0.15 MeV, and the uncertainty in the determination of the average energy was about 0.1 MeV.

Anisotropies from neutron-induced fission are presented in Fig. 1 for the even-even target nuclei and in Figs. 2–4 and 6 for the odd targets. The data are in good agreement with previous results[1–3] for several energies and fission sources where results of comparable accuracy are available. However, the present anisotropy for $n+Pu^{239}$ at $E_n \approx 11$ MeV is about 6% larger than our previously reported result[1] at $E_n \approx 11.1$ MeV. The probable cause of this discrepancy is that the effect of background neutrons was underestimated in the earlier data, for which no background measurements were made at this energy. Anisotropies for alpha-particle-induced fission of Th^{232} and U^{236} measured by the catcher foil method are presented in Figs. 3 and 4.

B. Semiconductor Detector Data

Anisotropy results for alpha-particle-induced fission of Th^{230}, Th^{232}, U^{233}, U^{235}, U^{236}, and U^{238} are presented in Table III and for deuteron-induced fission of U^{236} and Np^{237} in Table IV. The data have been corrected for (1) background fissions from Cf^{252} contamination on the counters, (2) transformation from laboratory to c.m. cross sections resulting in a 10 to 12% correction to the measured anisotropy for the alpha-particle data and a 4 to 6% correction for the deuteron data, and (3) solid angle factors for the $\theta=174°$ counters relative to the $\theta=90°$ counters as measured by Cf^{252} spontaneous fissions. Uncertainties in the data arise from counting statistics, uncertainty in the Cf^{252} calibration of 0.5% (2 to 4% for the 16.0- and 16.5-MeV measurements with the larger solid angles), statistical background un-

TABLE III. Fragment anisotropy $W(174°)/W(90°)$ for alpha-particle-induced fission observed by semiconductor detectors.

Alpha-particle energy (MeV)	Th^{230}	Th^{232}	U^{233}	U^{235}	U^{236}	U^{238}
16.0		1.087±0.082				
16.5		1.141±0.072			1.179±0.073	
17.0		1.124±0.040			0.972±0.073	1.180±0.079
18.2		1.341±0.058	1.096±0.079		1.150±0.078	1.153±0.076
19.4	1.329±0.035	1.342±0.027	1.102±0.027	1.125±0.035	1.259±0.037	1.222±0.030
21.0	1.290±0.029	1.271±0.025	1.141±0.024	1.120±0.032	1.222±0.057	1.212±0.025
22.0	1.262±0.028	1.278±0.026	1.132±0.024	1.140±0.024	1.221±0.044	
23.0	1.286±0.027	1.304±0.026	1.157±0.024	1.161±0.023	1.211±0.034	1.200±0.024
25.0	1.395±0.029	1.556±0.031	1.177±0.024	1.200±0.025	1.252±0.031	1.301±0.026
27.0	1.571±0.033	1.685±0.034	1.249±0.026	1.266±0.026	1.360±0.027	1.379±0.028
29.0	1.594±0.033	1.670±0.033	1.286±0.026	1.314±0.026	1.403±0.028	1.398±0.028

[32] J. A. Northrop and R. H. Stokes, Rev. Sci. Instr. **29**, 287 (1958).

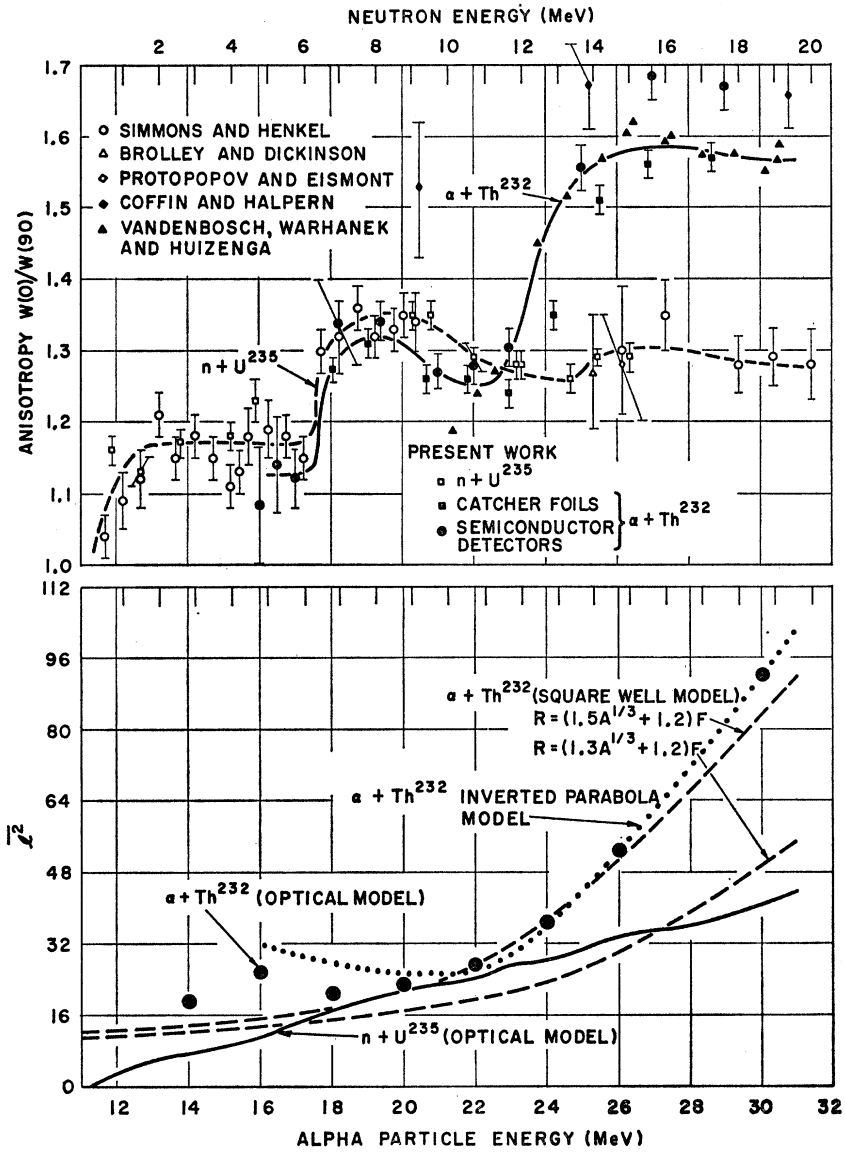

FIG. 3. Anisotropy data of fragments from the compound nucleus U^{236} and, below, orbital angular momentum calculations. Curves in the upper figure are not fits to data. See Refs. 2–5 for earlier data. The angles for the present measurements were actually 6° and 93° for semiconductor detector data, 9° and 91° for neutrons, and are given in Sec. IIA of the text for the catcher foil data. The calculations in the lower figure were based on: square-well method of Ref. 43 with a well depth of −50 MeV; alpha-particle optical model from Ref. 20 (also see Ref. 41); neutron optical model, parameters extrapolated from Ref. 16; and inverted parabola model calculated by the method of Ref. 39. The ordinate of the lower figure is $\langle l^2 \rangle_{av}$.

certainty, estimates of uncertainties in total counts resulting from overlap of the alpha-particle pileup and fission-fragment energy spectra, and about 2% from variation of the position of the beam spot on the target. The last uncertainty was determined from the differences in anisotropy produced by 90° changes in the target orientation. The uncertainties from overlap of alpha pileup and fragment pulses were $<0.4\%$ for the $E_\alpha > 23$-MeV data, in the range 0.1 to 4.5% for the $21 \leqq E_\alpha \leqq 23$-MeV data, from 0.4 to 6.4% for alpha-particle irradiations in the energy range $16 \leqq E_\alpha \leqq 19.4$ MeV, and $<1.2\%$ for the deuteron irradiations.

TABLE IV. Fragment anisotropy $W(174°)/W(90°)$ for deuteron-induced fission measured by semiconductor detectors.

Deuteron energy (MeV)	U^{236}	Np^{237}
8.6	1.096±0.027	1.076±0.024
9.5	1.094±0.025	1.071±0.022
10.6	1.118±0.025	1.085±0.022
11.5	1.133±0.024	1.093±0.023
12.6	1.153±0.025	1.097±0.023
13.5	1.164±0.024	1.118±0.023
14.45	1.183±0.026	1.129±0.023

The anisotropies are presented in Figs. 2–7 and generally agree with previous results[4–6] and with data obtained by the catcher foil method. However, the semiconductor detector data for $\alpha + Th^{232}$ at $E_\alpha = 27$ and 29 MeV in Fig. 3 appear about 6% larger than the Vandenbosch *et al.*[4] data and catcher foil results; all semiconductor detector data are generally larger than

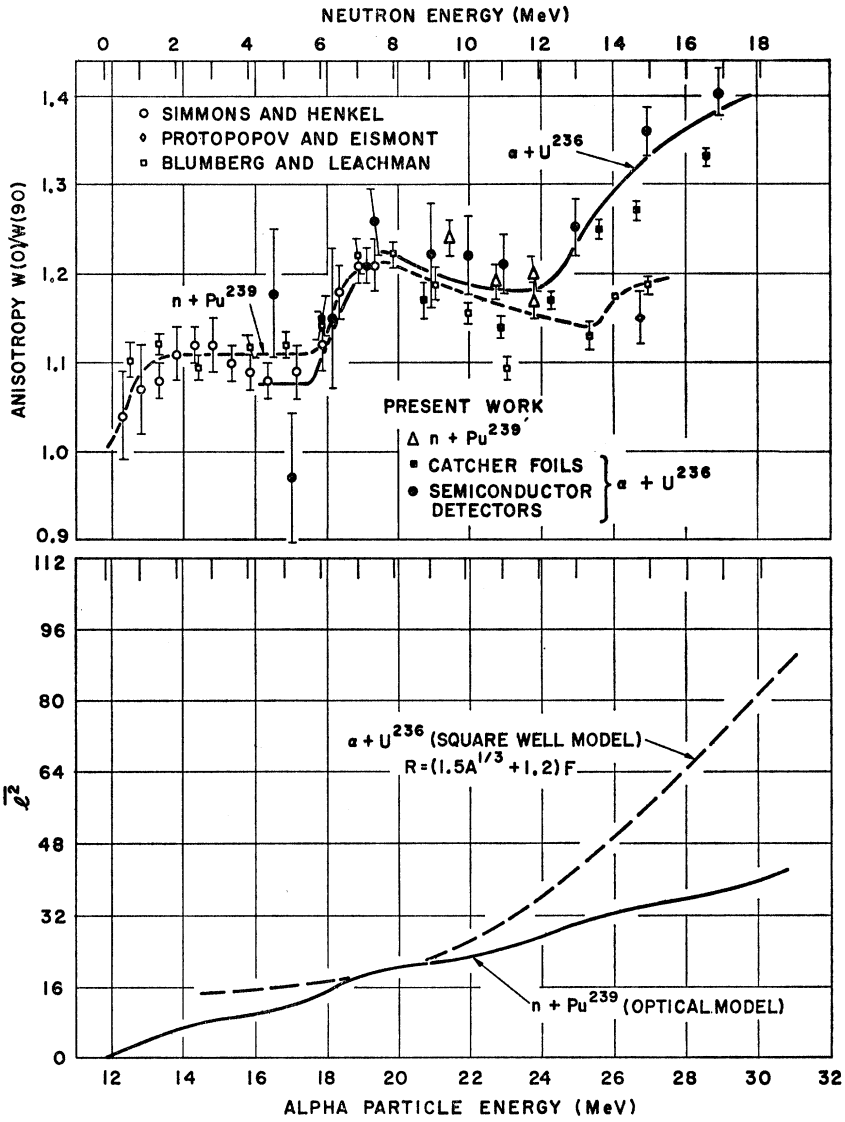

FIG. 4. Anisotropy data of fragments from the compound nucleus Pu^{240} and, below, orbital angular momentum calculations. See the caption to Fig. 3 for other details. See Refs. 1–3 for earlier data. Curves in the upper figure are not fits to data.

the catcher foil data for energies $E_\alpha > 23$ MeV. Also, there is an unexplained systematic difference of about 3 to 8% between the semiconductor detector and catcher foil data for the $\alpha+U^{236}$ data of Fig. 4. The present semiconductor data in Tables III and IV are in excellent agreement with the $\alpha+U^{233}$ and $\alpha+U^{238}$ anisotropies of Vandenbosch *et al.*[4] and with the published $d+Np^{237}$ anisotropies[5,6] and the $d+U^{236}$ anisotropy.[6]

The energy scales in Figs. 2–7 have been translated to present the different particle-induced anisotropies at the same excitation energy of the compound nucleus.[33]

IV. DISCUSSION

The anisotropies of alpha-particle-induced fission clearly show step-like increases at the approximately 17-MeV onset of (α,nf) fission in Figs. 3–5 and the approximately 23-MeV onset of $(\alpha,2nf)$ fission in Figs. 2–5. This is an expected, but previously unobserved, result that is in accord with less distinct steps in anisotropy at higher energies[4] and with the $(\alpha,2nf)$ dip in the peak-to-valley ratio of mass yield.[18] For neutron-induced fission, rises in the anisotropy[1,2,7] and in the cross section[34] have been observed from this cause, and for proton-induced fission dips in the valley-to-peak ratio of mass yield have been observed.[35,36,36a]

[33] Masses used were from A. H. Wapstra, in *Handbuch der Physik*, edited by S. Flügge (Springer-Verlag, Berlin, 1958), Vol. 38/1, p. 1.

[34] W. D. Allen and R. L. Henkel, *Progress in Nuclear Energy* (Pergamon Press, Inc., London, 1958), Ser. 1, Vol. 2, p. 1.

[35] G. R. Choppin, J. R. Meriwether, and J. D. Fox, Phys. Rev. **131**, 2149 (1963).

[36] B. J. Bowles, F. Brown, and J. P. Butler, Phys. Rev. **107**, 751 (1957) and J. P. Butler, B. J. Bowles, and F. Brown, in *Proceedings of the Second International Conference on the Peaceful Uses of Atomic Energy, Geneva, 1958* (United Nations, Geneva, 1959), Vol. 15, p. 156.

[36a] *Note added in proof.* J. E. Gindler, G. L. Bate, and J. R. Huizenga, Phys. Rev. **136**, B1333 (1964), observe a distinct step in anisotropy of $\alpha+Ra^{226}$ fission at the onset of $(\alpha,2nf)$ fission.]

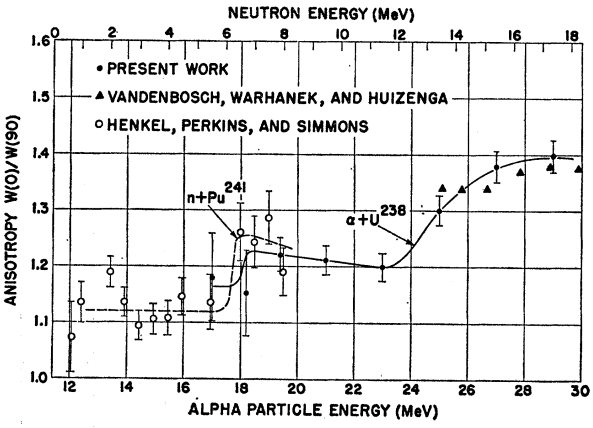

FIG. 5. Anisotropy data of fragments from the compound nucleus Pu^{242}. Curves are not fits to data. See Refs. 4 and 7 for the other data shown. The angles for the present data were actually 6° and 93°.

It should be noted that the use of Eq. (1) at the higher energies where (α,xnf) fission occurs implies the use of a K_0^2 averaged over the different fission processes which result from prefission neutron emission. Prefission neutrons are assumed not to change I^2 significantly. The average $\langle K_0^2\rangle$ of K_0^2 with respect to the relative probabilities of (α,f), (α,nf), and $(\alpha,2nf)$ processes can differ significantly from the K_0^2 that pertains only to the (α,f) process. However, we estimate that the *relative* change in $\langle K_0^2\rangle$ for irradiations with alpha particles compared to neutrons, with both resulting in the same compound nucleus and excitation energy, is at most 2.2% in the cases we consider and thus is small compared to the uncertainties in comparisons of anisotropy ratios below. Such relative $\langle K_0^2\rangle$ changes result from an I-dependent fissionability as in Eq. (2).

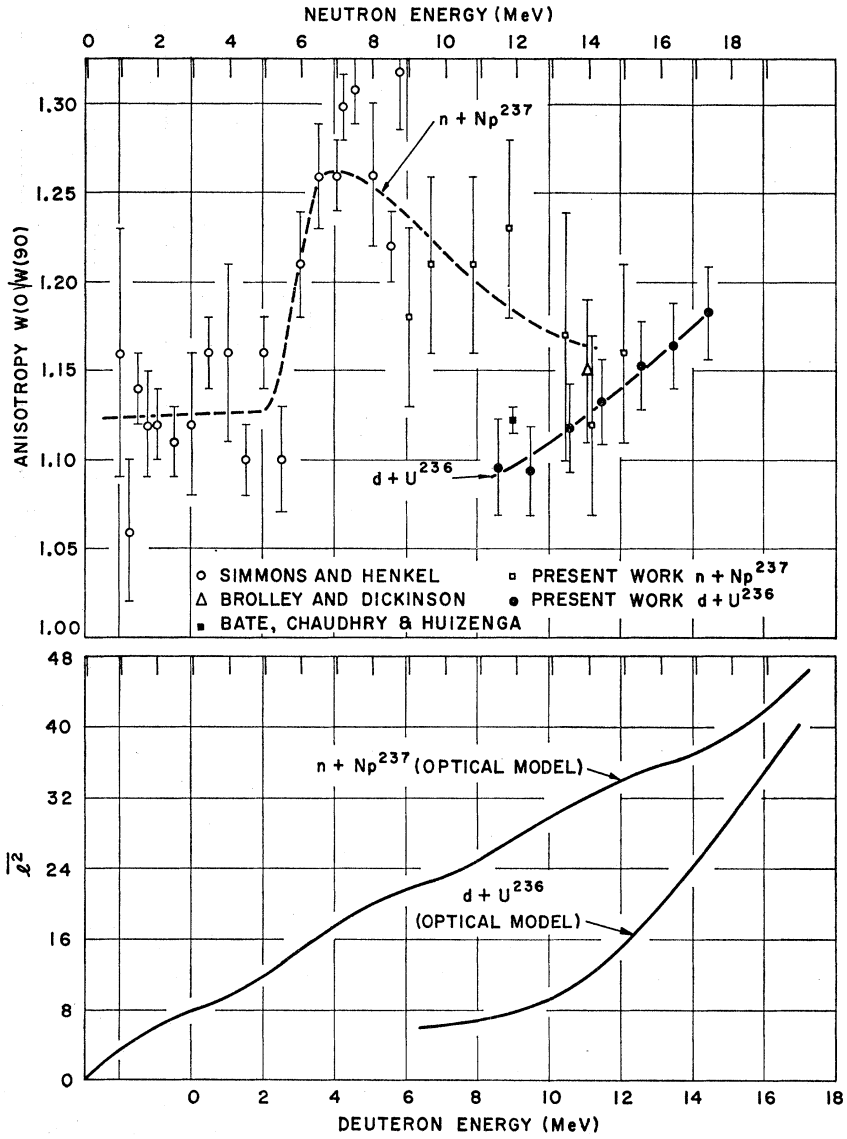

FIG. 6. Anisotropy data of fragments from the compound nucleus Np^{238} and, below, orbital angular momentum calculations. Curves in the upper figure are not fits to the data. The angles for the present data were actually 6° for deuterons and 9° and 91° for neutrons. Deuteron optical model parameters are in Ref. 38; neutron optical parameters were extrapolated from Ref. 16. See Refs. 2, 3, and 6 for earlier data.

A. Dependence of K_0 upon Angular Momentum

We now test whether K_0 is independent of I and the identity of the bombarding particle by rewriting Eq. (1) as

$$\left[\frac{W(0)}{W(90)}-1\right]_\alpha \Big/ \left[\frac{W(0)}{W(90)}-1\right]_n = \langle l_\alpha^2\rangle_{\rm av}/\langle l_n^2\rangle_{\rm av}, \quad (3)$$

where the subscripts are for alpha particles and neutrons and terms dependent upon the target spin I_0 have been neglected. [See (1) of Sec. I.]

Shown in Figs. 3, 4, 6, and 7 are calculations of $\langle l^2\rangle_{\rm av}$. The calculated $\langle l_n^2\rangle_{\rm av}$ for neutrons result from the use of optical model parameters extrapolated from those obtained by Beyster *et al.*[16] The parameters of Bjorklund and Fernbach[37] were found to give essentially the same results, just as does the classical $\langle l_n^2\rangle_{\rm av}=2.26\ mE_n$ obtained from the reasonable value of the radius $R=1.57\ A^{1/3}$F with m in atomic mass units, A the target mass number, and E_n in mega-electron volts. The $\langle l_\alpha^2\rangle_{\rm av}$ results in Figs. 6 and 7 are from the use of the optical model parameters of Miller *et al.*[38]

At higher energies (greater than ~22 MeV), the optical model calculations of $\langle l_\alpha^2\rangle_{\rm av}$ based on T_l values from Huizenga and Igo[20] agree with the square well calculations[15] when a well depth of −50 MeV and a radius $R=(1.5A^{1/3}+1.2)$F are used (Fig. 3). Both result from fits to data, the former from fits to angular distributions and reaction cross sections and the latter from fits to reaction cross sections σ_r.[17,18] [The smaller radius $R=(1.3A^{1/3}+1.2)$F does not give agreement[17,18] with measured reaction cross sections, and so the greatly different $\langle l_\alpha^2\rangle_{\rm av}$ values in Fig. 3 calculated from this radius can be rejected.] In Fig. 3 is also shown the result of a calculation[39] of $\langle l_\alpha^2\rangle_{\rm av}$ from the model of inverted parabolas[40] fitted to the maxima of the potential barriers for the different orbital angular momenta l. The parabolas were matched to the barriers obtained from the use of the Huizenga-Igo optical model parameters,[20] and so it is not surprising that these $\langle l_\alpha^2\rangle_{\rm av}$ results match the optical model results at our highest energies.

We now make comparisons between the calculated angular momenta and anisotropy by means of Eq. (3). The $\langle l_\alpha^2\rangle_{\rm av}$ calculations appear to be accurate above $E_\alpha\approx 22$ MeV, but comparisons are most reliable for the $E_\alpha\geq 27$-MeV region where anisotropies do not change rapidly with energy. In the comparisons, optical model values of $\langle l^2{}_\alpha\rangle_{\rm av}/\langle l^2{}_n\rangle_{\rm av}$ were used, and anisotropies from Figs. 2–4 were expressed by the left-hand side of Eq. (3). These values are, respectively: for the U^{234} compound nucleus in Fig. 2 (angular momenta not illustrated), 2.2 and 2.6±0.6 at $E_\alpha\approx 29$ MeV; for the U^{236} compound nucleus in Fig. 3, 1.9 and 2.0±0.1 at $E_\alpha\approx 27$ MeV and 2.1 and 2.1±0.3 at $E_\alpha\approx 29$ MeV; and for the Pu^{240} compound nucleus in Fig. 4 (optical-model calculation of $\langle l^2{}_\alpha\rangle_{\rm av}$ not illustrated), 1.7 and 1.5±0.1. The agreements between these values for the two sides of Eq. (3) indicate no serious error in the assumption of K_0 being independent of I and the identity of the bombarding particle.

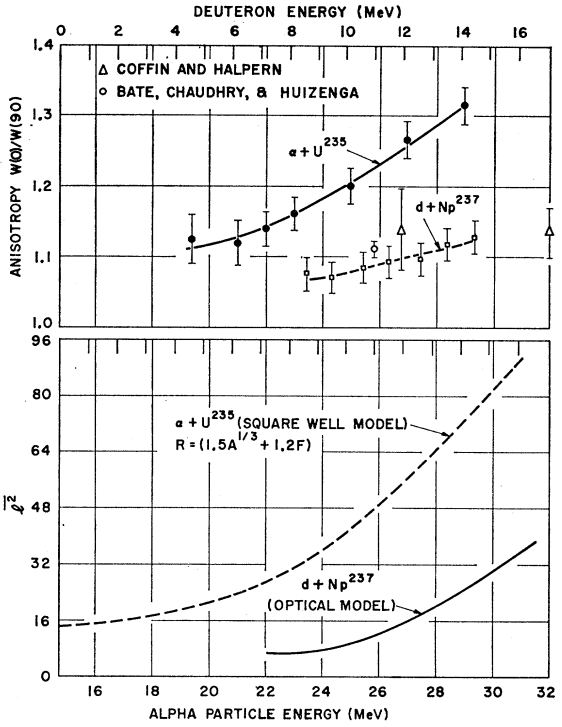

FIG. 7. Anisotropy data of fragments from the compound nucleus Pu^{239} and, below, orbital angular momentum calculations. Alpha-particle square-well calculations are from the method of Ref. 43 with a well depth of −50 MeV; deuteron optical model parameters are in Ref. 38. See Refs. 5 and 6 for earlier data. Curves in the upper figure are not fits to the data. The 0° angle of the present data was actually 6°, and the 90° angle for alpha-particle data was 93°.

B. Orbital Angular-Momentum Comparisons with Anisotropy

We now use Eq. (3) with the experimental data to investigate the calculated $\langle l^2{}_\alpha\rangle_{\rm av}$ for alpha-particle energies below about 22 MeV. The results in Fig. 3 show that the inverted parabola method[39] is too approximate and results in $\langle l^2{}_\alpha\rangle_{\rm av}$ values that are too large in this low-energy region. For the 16-MeV region of alpha-particle energies, the $\langle l^2{}_\alpha\rangle_{\rm av}$ values from optical model calculation[20,41] are clearly seen from Fig. 3 to be

[37] F. Bjorklund and S. Fernbach, Phys. Rev. **109**, 1295 (1958).
[38] D. W. Miller, H. E. Wegner, and W. S. Hall, Phys. Rev. **125**, 2054 (1962).
[39] Kindly made with the BUNTHORNE code [T. D. Thomas, Phys. Rev. **116**, 703 (1959)] by J. O. Rasmussen and R. Kiefer.
[40] D. L. Hill and J. A. Wheeler, Phys. Rev. **89**, 1102 (1953).
[41] In a private communication, Huizenga suspects the calculated values in Ref. 20 to be in error below 18 MeV. R. J. McKee has used these optical-model parameters in the M. A. Melkanoff SCAT code and calculated $\langle l_\alpha^2\rangle_{\rm av}\approx 27$ from 14 to 20 MeV. Thus, both these optical-model $\langle l_\alpha^2\rangle_{\rm av}$ results in this energy region are considerably higher than square-well calculations and the data.

too large; here, $\langle l^2_\alpha\rangle_{\rm av}/\langle l^2_n\rangle_{\rm av}=1.9$ is much larger than the corresponding [left-hand side of Eq. (3)] anisotropy value of 0.6 ± 0.1 obtained from a weighted average of $Th^{232}(\alpha,f)$ data at 16, 16.5, and 17 MeV and $U^{235}(n,f)$ data at 4.7, 5.0, and 5.5 MeV. A possible explanation[42] is that optical-model codes commonly contain Coulomb routines which are inadequate for these low-energy cases where the Coulomb parameter $\eta=Z_1Z_2e^2/\hbar v\approx14.5$. However, the Coulomb routine for our square-well calculations by Gursky[43] allows these large η values, and with Eq. (3) the agreement between experiment and these $\langle l^2\rangle_{\rm av}$ calculations is considerably improved.

The η values for deuteron energies in Figs. 6 and 7 are adequately low for valid calculations with optical model codes, and the limited comparison with anisotropy measurements are satisfactory, especially for the $\alpha+U^{235}$ and $d+Np^{237}$ comparison of the compound nucleus Pu^{239} in Fig. 7. This indicates that fission is induced principally by the full capture of the deuteron.[44] The agreement between anisotropy ratios and ratios of calculated $\langle l^2\rangle_{\rm av}$ values at the higher energies for the Np^{238} compound nucleus in Fig. 6 is not good, but the uncertainties in the anisotropy data are large.

It is interesting to attempt a qualitative understanding of the shape of the $\langle l^2_\alpha\rangle_{\rm av}$ calculations in Figs. 3 and 4. First considering the higher energies, we find that the calculated $\langle l^2_\alpha\rangle_{\rm av}$ values increase nearly linearly with energy, just as is qualitatively expected from a classical consideration[9] of the transmission coefficients T_l being either unity or zero depending on the wavelength criterion.[45] For lower energies, Jauho has noted[19] that the present investigation provides the possibility of understanding penetrations from the WKB approximation over a larger span of alpha-particle energies than has been used for alpha particles of radioactive decay. We thus apply the WKB approximation for $E_\alpha\leqq18$ MeV, where nearly constant $\langle l^2\rangle_{\rm av}$ values shown in Fig. 3 are accurately calculated by the square-well model and are confirmed by the anisotropy data.

The approximation $V_l\ll V_c-E_\alpha$, where $V_l=\hbar^2l(l+1)/2m_\alpha r^2$ is the centrifugal potential and V_c is the Coulomb potential, is used in the exponential part of a WKB approximation[46] for the transmission coefficient

$$T_l\propto\exp\{-2\int[(2m/\hbar^2)(V_l+V_c-E_\alpha)]^{1/2}dr\}.$$

Then the relative transmission coefficients for two orbital angular momenta i and j are

$$\frac{T_i}{T_j}\approx\exp\left\{\int_R^\rho\left(\frac{2m_\alpha}{\hbar^2}\right)^{1/2}\frac{V_j-V_i}{(V_c-E_\alpha)^{1/2}}dr\right\}, \qquad (4)$$

where ρ is the classical turning point radius. Since $\hbar^2/2m_\alpha R^2$ is roughly 0.05 MeV and $V_c(R)-E_\alpha$ is between 10 and 28 MeV for the 0–18-MeV E_α of interest, Eq. (4) indicates two relevant facts: first, $(T_i/T_j)\sim1$, because the exponential in Eq. (4) is small for the orbital angular momenta l of interest; and, second, as $E_\alpha\to0$, the E_α dependence of T_i/T_j vanishes. The first makes understandable the rather large $\langle l^2_\alpha\rangle_{\rm av}$ values in this energy region, and the second explains why $\langle l^2_\alpha\rangle_{\rm av}$ decreases only slightly with E_α. These properties for low-energy charged particles are implicit in previous discussions.[47] In exact calculations, McHale[48] finds $\langle l^2_\alpha\rangle_{\rm av}\to8.6$ as $E_\alpha\to0$ for the same $V_0=-50$ MeV and $R=(1.5A^{1/3}+1.2)$F of the square-well calculation[43] that gives $\langle l^2_\alpha\rangle_{\rm av}=9.9$ at $E_\alpha=8$ MeV. Thus calculations indicate $\langle l^2_\alpha\rangle_{\rm av}\approx9$ through this energy region (below the Fig. 3 energy region), in agreement with various WKB calculations[49] for radioactively emitted alpha particles.

C. Dependence of Anisotropy upon Target Spin

Finally, we consider the comparisons in Figs. 3–5 of anisotropy in the lowest energy region of exclusively (α,f) and (n,f) fissions. Here, Eq. (1) can be applied directly without complications from (α,nf), $(n,n'f)$, etc., fission. In principle, Eq. (1) can be used with the anisotropy data and the calculated $\langle l^2_n\rangle_{\rm av}$ and $\langle l^2_\alpha\rangle_{\rm av}$ values to ascertain the moment of inertia parameter $\mathfrak{A}$, given by Eq. (2), from a ratio equation analogous to Eq. (3) but containing the target spin terms of Eq. (1). In practice, however, the calculated $\langle l^2\rangle_{\rm av}$ values are too uncertain.

Owing to this uncertainty, we analyze the target spin effects in this energy region by a simple method that assumes only that $\langle l^2\rangle_{\rm av}$ varies little from target to target. To see if the anisotropies can be understood with all target spin terms in Eq. (1) neglected and so only changes in K_0 from compound nucleus to compound nucleus entering, we simply compare the difference between the neutron-induced fission anisotropies of U^{235} and Pu^{239} with the difference between the corresponding alpha-induced fission anisotropies of Th^{232} and U^{236}. Unfortunately, the low counting rate and the corrections for the low-energy tails extending into the fission spectra resulted in large uncertainties in the anisotropy from alpha-particle-induced fission, and so a weighted average of the 16.5- and 17-MeV data is used. Then, the dif-

[42] R. M. Drisko, M. L. Gursky, and M. A. Melkanoff (private communications).
[43] M. L. Gursky (private communication); calculations based on the infinite square-well model of Blatt and Weisskopf, Ref. 14. We are grateful to Dr. Gursky for these calculations.
[44] This has been observed at higher deuteron energies by W. J. Nicholson and I. Halpern, Phys. Rev. **116**, 175 (1959) and T. Sikkeland, E. L. Haines, and V. E. Viola, Jr., *ibid.* **125**, 1350 (1962).
[45] J. S. Blair, Phys. Rev. **95**, 1218 (1954).
[46] Reference 14, p. 573.
[47] M. Ostrofsky, G. Breit, and D. P. Johnson, Phys. Rev. **49**, 22 (1936); and E. P. Wigner, *ibid.* **73**, 1002 (1948).
[48] J. L. McHale, Jr. (private communication). We are grateful to Dr. McHale for these calculations.
[49] I. Perlman and J. O. Rasmussen, in *Handbuch der Physik*, edited by S. Flügge (Springer-Verlag, Berlin, 1957), Vol. 42, p. 109.

ference for alpha-particle-induced fission is 0.052 $\pm$0.062, while the difference for neutron-induced fission is 0.066$\pm$0.022. Thus, within an uncertainty as large as the effect itself, the difference between the anisotropies of the compound nuclei U^{236} and Pu^{240} can be entirely due to the moment of inertia $\mathcal{I}_{\text{eff}}$ change (change in K_0^2), since the same difference is obtained for the neutron-induced case involving a target spin difference as for the spinless case of alpha-particle-induced fission. This conforms to the results of Simmons *et al.*[7] obtained from systematics of K_0 as a function of Z^2/A of the fissioning nucleus. The anisotropies for the compound nucleus Pu^{242} in Fig. 5 obtained by $\alpha+U^{238}$ and $n+Pu^{241}$ ($I_0=\frac{5}{2}$) lack adequate accuracy for a similar comparison.

The accuracy of the present results does not, however, argue against changes in anisotropy with target spin resulting from fissionability effects [last term in Eq. (1)] when reasonable values of moments of inertia $\mathcal{I}_n$ are used in Eq. (2), but do argue against the necessity of unreasonably small $\mathcal{I}_n$ to explain the data from neutron-induced fission.

V. CONCLUSIONS

Data at our higher energies confirm that K_0, and thus the effective moment of inertia $\mathcal{I}_{\text{eff}}$ of saddle-point nuclei, is independent of the angular momentum I and of the identity of the particle inducing fission. At our lower energies we find that generally used optical-model codes do not calculate transmission coefficients T_l accurately, but that an accurate code of the square-well model with a $V=-50$-MeV well and a radius $R=(1.5A^{1/3}+1.2)$F agrees with the anisotropy data. Data at our lowest energies of alpha particles indicate that the previously observed increase in anisotropy for $n+U^{235}$ compared to $n+Pu^{239}$ can largely be due to changes in K_0, and thus to changes in the effective moment of inertia $\mathcal{I}_{\text{eff}}$, rather than to unexplained effects of target spin I_0 as had been believed.

ACKNOWLEDGMENTS

We wish to thank J. J. Griffin for discussions on the theory of fission angular distributions and D. C. Dodder for discussions on Coulomb barrier penetration. Thanks are due J. Gursky, J. Povelites, and P. Stein for the many fission sources, foil backings, and windows used as well as developmental work on the electro-spraying method of target preparation. We are grateful to D. D. Armstrong, R. W. Davis, and R. K. Smith for assistance in accelerator operation. The optical model and potential-well model codes were kindly made available by M. L. Gursky with computational assistance from M. Peacock, R. McKee, and J. Matthews.